Developmental Biology 367 (2012) 126–139

Contents lists available at SciVerse ScienceDirect

Developmental Biology

journal homepage: www.elsevier.com/locate/developmentalbiology

Chemoattractant axon guidance cues regulate *de novo* axon trajectories in the embryonic forebrain of zebrafish

Arnaud Gaudin, Wolfgang Hofmeister, Brian Key *

Brain Growth and Regeneration Lab, School of Biomedical Sciences, The University of Queensland, Brisbane 4072, Queensland, Australia

ARTICLE INFO

Article history:
Received 29 October 2011
Received in revised form
24 April 2012
Accepted 25 April 2012
Available online 8 May 2012

Keywords:
Axon guidance
Zebrafish
Dcc
Netrin
Commissure

ABSTRACT

The development of axon tracts in the early vertebrate brain is controlled by combinations of soluble, membrane-bound and extracellular matrix molecules. How these multiple and sometimes conflicting guidance cues are integrated in order to establish stereotypical pathways remains to be determined. We show here that when interactions between the chemoattractive signal Netrin1a and its receptor Dcc are suppressed using a loss-of-function approach, a novel axon trajectory emerges in the dorsal diencephalon. Axons arising from a subpopulation of telencephalic neurons failed to project rostrally into the anterior commissure in the absence of either Netrin1a or Dcc. Instead these axons inappropriately exited the telencephalon and ectopically coursed caudally into virgin neuroepithelium. This response was highly specific since loss-of-function of Netrin1b, a paralogue of Netrin1a, generated a distinct phenotype in the rostral brain. These results show that a subpopulation of telencephalic neurons, when freed from long-range chemoattraction mediated by Netrin1a–Dcc interactions, follow alternative instructive cues that lead to creation of an ectopic axon bundle in the diencephalon. This work provides insight into how integration of multiple guidance signals defines the initial scaffold of axon tracts in the embryonic vertebrate forebrain.

Introduction

How do the chemoattractant axon guidance molecules (such as Netrins, Shh, Vegf, Semaphorins, Fgf, Gdnf and Wnt) lead to the formation of a stereotypical set of axon tracts in the developing vertebrate brain? While the question of neuronal specificity in regard to the topography of the retinotectal pathway (Sperry, 1963) seems to be now understood in terms of gradients of a small number of guidance cues, it remains unclear how the initial template of axon tracts is established within the forebrain. Although it has been largely accepted that navigation of axons is governed by combinations of short- and long-range attractive and repulsive cues (Tessier-Lavigne and Goodman, 1996), the relative contribution of multiple guidance systems to the establishment of a specific tract is not yet understood. With so many guidance cues expressed in relatively small and partially overlapping areas in the embryonic brain, growth cones must integrate and balance redundant and opposing instructions to establish stereotypical pathways. What happens to the formation of the initial template of axon tracts in the embryonic forebrain when we remove the attraction of a single guidance system? Will other cues compensate for the loss of this system or will they steer the axons in a different direction?

dcc (deleted in colon cancer) was initially identified as a gene on chromosome 18 which was deleted in colorectal carcinomas and thought to be a tumour suppressor (Fearon et al., 1990). *dcc* was subsequently reported to be strongly expressed in the vertebrate nervous system (Lawlor and Narayanan, 1992) where it acted as a chemoattractant receptor for the netrin family of soluble ligands (Keino-Masu et al., 1996). Much of what is now known about the role of *dcc*/*netrin* in the developing nervous system pertains to late stages of maturation involving enlargement of pre-existing tracts. In the mouse, knock out of either *dcc* or *netrin1* causes defects in the corpus callosum and the anterior and hippocampal commissures. Interestingly, the dorsal commissures (habenular and posterior commissures) were largely unaffected (Serafini et al., 1996; Fazeli et al., 1997). In order to better understand how chemoattractant axon guidance molecules contribute to the initial formation of axon tracts, we have reassessed the role of Dcc and its Netrin1 ligands during early embryonic forebrain development in zebrafish.

The first axon tracts in the early vertebrate forebrain are organised stereotypically (Anderson and Key, 1999; Ware and Schubert, 2011; Easter et al., 1993). For instance, by 30 h post fertilisation (hpf) in zebrafish, the forebrain consists of five

* Corresponding author.
E-mail addresses: a.gaudin@uq.edu.au (A. Gaudin), w.hofmeister@uq.edu.au (W. Hofmeister), brian.key@uq.edu.au (B. Key).

0012-1606/$ - see front matter © 2012 Elsevier Inc. All rights reserved.
http://dx.doi.org/10.1016/j.ydbio.2012.04.032

neuronal clusters interconnected by seven axon tracts (Wilson et al., 1990; Chitnis and Kuwada, 1990; Ross et al., 1992). Each of these nuclei and tracts form in a well described sequence from 17 hpf (Fig. 1). Despite a clear description of the neuroanatomy of these early tracts, very little is understood about the molecular and cellular bases of their formation. *dcc* mRNA is detected in the telencephalon at 18 hpf, in the caudal portion of the dorsorostral cluster of neurons in the telencephalon (Hjorth et al., 2001; Fricke and Chien, 2005). While all the major neuronal clusters in the forebrain express *dcc* at 24 hpf, the strongest expression continues to be localised in the caudal portion of the dorsorostral cluster. By 30 hpf, the expression of *dcc* in the forebrain is greatly reduced and is barely detectable in the telencephalon. *dcc* is therefore dynamically expressed in a tightly regulated spatiotemporal pattern in the forebrain during the early establishment of the axon scaffold. *netrin1a* (Lauderdale et al., 1997) and *netrin1b* (Strähle et al., 1997) are two paralogues homologous to the mouse *netrin1* (Gates et al., 1999). They most likely arose from a gene duplication that happened early in the teleost lineage (Meyer and Malaga-Trillo, 1999, Postlethwait, 2007). The expression pattern of each paralogue differs in several regions of the nervous system (Strähle et al., 1997; Lauderdale et al., 1997),
a common phenomenon for paralogues resulting from whole genome duplication events (Kassahn et al., 2009). While Dcc–Netrin interactions mediate axon guidance in select zebrafish brain regions (Suli et al., 2006; Kastenhuber et al., 2009), their role in the earliest stages of axon tract formation in the rostral brain remains unknown.

We have examined here the role of Dcc–Netrin1 interactions in the development of the early template of axon tracts in the vertebrate forebrain. We report that loss of function of either *dcc* or *netrin1a* results in misguidance of axons that normally project into the anterior commissure in embryonic zebrafish. The misguided axons, rather than wandering randomly, followed a stereotypical route, forming an ectopic axon bundle that emerged caudally from the telencephalon and extended into the diencephalon. We also report the expression pattern of both netrin1 paralogues at the commissural plate and reveal distinct roles of these molecules in formation of the anterior commissure. Our results provide insights into mechanisms of formation of *de novo* axon trajectories during development.

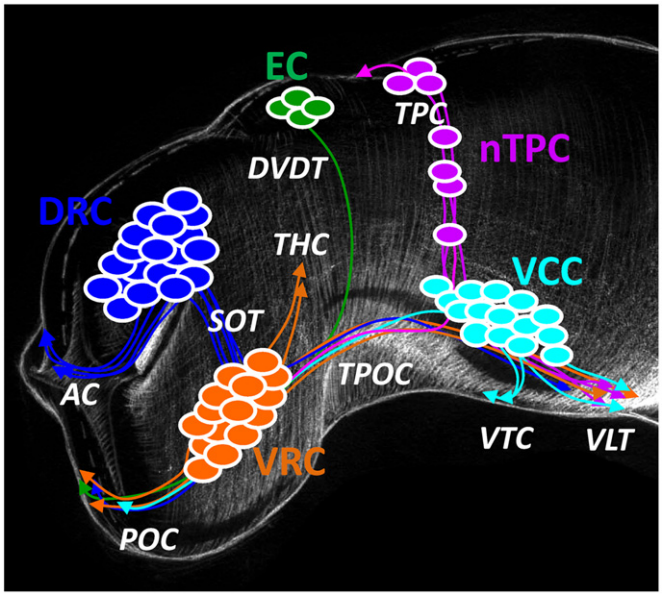

Fig. 1. *Principal neuronal clusters and axon tracts in the embryonic zebrafish brain.* This diagram represents an anterolateral view of the zebrafish forebrain at 30 h post fertilisation. Anterior is left, dorsal is up. The neuronal clusters are represented in different colours and the axons that are typically known to be related to them are coloured accordingly. During development, the first cluster of neurons to differentiate is the mesencephalic ventro-caudal cluster (VCC in light blue) around 16 hpf. The ventral longitudinal tract (VLT) extends caudally from the VCC towards the posterior parts of the brain around 17 hpf. The next cluster to differentiate is the diencephalic ventrorostral cluster (VRC in orange) around 17 hpf. The tract of the post-optic commissure (TPOC) is formed by axons extending caudally from the VRC towards the VCC at 18 hpf. The VRC also sends axons rostrally to form the post-optic commissure (POC) from 20 hpf onwards. By then, the telencephalic dorsorostral cluster (DRC, in dark blue) has also started to send axons ventrally via the supra-optic tract (SOT). The fibres descending via the SOT will continue their course either through the TPOC or the POC. Two other dorsal clusters will also start extending fibres ventrally from 20 hpf onwards: the diencephalic epiphyseal cluster (EC, in green) sends axons ventrally through the dorsoventral diencephalic tract (DVDT) that will merge with the TPOC and continue through the POC to the contralateral diencephalon; and the mesencephalic nucleus of the tract of the posterior commissure (nTPC, in pink) will constitute both the tract of the posterior commissure (TPC) and the dorsal mesencephalic posterior commissure (PC). Around 24 hpf, axons from the DRC form the anterior commissure in the rostral telencephalon. Shortly after at ~28 hpf, the tract of the habenular commissure (THC) starts extending from the ventral diencephalon towards the dorsal diencephalon where it will later join the habenular commissure, lying rostral to the EC. Based on Chitnis and Kuwada (1990), Wilson et al. (1990) and Ross et al. (1992).

Material and methods

Fish stocks and embryo production

All fish lines were maintained on a 14-h light/10-h dark cycle and embryos were generated by natural spawnings. The *Tg*(*elavl3*:*kaede*)^{rw0130a} transgenic line (also known as *HuC*:*kaede*; Sato et al., 2006) was a kind gift of Hitoshi Okamoto (RIKEN Brain Institute, Wako, Japan). We used *HuC*:*kaede* crossed with *Tg*(*foxd3*:*GFP*)*zf105* (referred as *FoxD3*:*GFP*) for the strong fluorescence they exhibit in the epiphysis and the DVDT (Gilmour et al., 2002). Embryos from natural spawnings were raised at 28.5 °C in E3 embryo medium supplemented with methylene blue and staged as previously described (Kimmel et al., 1995).

Morpholino injections

Translation blocking morpholino oligonucleotides (MO) were purchased from Gene Tools LLC (Philomath, Oregon). MO experiments have been conducted in accordance with standard guidelines (Moulton and Yan, 2008). MO stock solutions (10 ng/nL) were stored at room temperature in the original glass vial provided by Gene Tools LLC. We diluted the working solutions in distilled water extemporaneously. Working solutions were injected using a PV830 pneumatic Picopump (World Precision Instruments, Sarasota, Florida) into the yolk stream directly adjacent to the dividing cells between the 1 and 4 four-cell stage of development. All MO used in the present study have been previously demonstrated to selectively knock down their specific target. The sequences of the different MO were: *dcc*-ATG 5′-GAATATCTCCAGTGACGCAGCCCAT-3′, *dcc*-UTR 5′-GCGAAATCCGCTGCTAATCAATCAA-3′ (Suli et al., 2006; Kastenhuber et al., 2009; Lim et al., 2011), *netrin1a* 5′-ATGATGGACTTACCGACACATTCGT-3′ (Suli et al., 2006; Kastenhuber et al., 2009; Lim et al., 2011), *netrin1b* 5′-GCACGTTACCAAAATCCTTATCAT-3′ (Suli et al., 2006; Kastenhuber et al., 2009), *shh* 5′-CAGCACTCTCGTCAAAAGCCGCATT-3′ (Nasevicius and Ekker, 2000) and STD 5′-CCTCTTACCTCAGTTACAATTTATA-3′ (Gene Tools, LLC). Control animals for each experiment were either injected with an equivalent amount of the standard control MO or uninjected. We never observed any phenotypic effects of the control MO injected embryos when compared to uninjected embryos.

Cell death and acridine orange

To confirm that the phenotypes observed were due to the specific knock down rather than off-target cell death, we used an acridine orange test previously described (Tucker and Lardelli, 2007). Most MO knock downs did not exhibit a significantly higher labelling with acridine orange compared to controls when injected with less than 6 ng of the MO used in this study. Above such doses, embryos exhibited gross anatomy defects correlating with strong acridine orange staining and axon scaffold alteration. Such embryos were excluded from further analysis. Only those embryos which displayed a normal gross morphology were processed for subsequent analysis of the axon scaffold. This conservative approach excluded the possibility that axon guidance defects were generated indirectly by morphological defects not directly linked to the knock down.

Immunostaining

All embryos were fixed in 4% (w/v) paraformaldehyde in phosphate buffered saline (pH=7.4) for 15 h at 4 °C or at room temperature for two hours. Fixed brains were dissected using fine forceps ensuring that the skin around the forebrain was carefully removed prior to immunostaining. Brains were incubated one hour at room temperature in blocking solution consisting of 2% Bovine serum albumen in Tris buffered saline (TBS) with 0.3% Triton X-100 (Tx). Brains were then incubated in the primary antibody solution (mouse monoclonal IgG anti-acetylated alpha-tubulin diluted in 1:300 in blocking solution; Sigma-Aldrich, St Louis, Missouri) at 4 °C overnight. Samples were washed 4 × 15 min in TBS–Tx before applying the secondary antibody (goat anti-mouse IgG coupled with Texas red, Sigma-Aldrich) diluted 1:200 for 3 h at room temperature. Samples were then rapidly washed three times in TBS–Tx before mounting in polyvinyl alcohol (Valnes and Brandtzaeg, 1985) and imaging.

DiI labelling

An ABAB-501 iontophoresis pump (Kation Scientific, Minneapolis, Minnesota) was used to deliver DiI (1,1′-dioctadecyl-3,3,3′,3′-tetramethylindocarbocyanine perchlorate; Invitrogen, Carlsbad, California) into localised brain regions. DiI was diluted in absolute ethanol, loaded into a microinjection pipette and delivered onto the surface of the dissected and fixed brains under a current of approximately 1 μA. We stopped the application as soon as a deposit was visible at the tip of the needle. The brains were then stored at room temperature in phosphate buffered saline (PBS, pH 7.4) in the dark to allow migration of the dye for at least 3 h before imaging.

Kaede photoconversion

Live *HuC*:*kaede* embryos injected with 3 ng of either standard control or *dcc* MO were anaesthetised in 0.01% tricaine methanesulfonate (Sigma Aldrich) before being mounted in a glass bottom petri dish in 1% agarose. Embryos were oriented so that the dorsal part of the dorsorostral cluster in the telencephalon was positioned towards the surface of the petri dish. The embryos were then examined using an IX81 confocal microscope (Olympus, Tokyo, Japan). Photoconversion was achieved by short laser pulses (2 s pulses, 405 nm at 80% output power) on the target portion of the brain (Sato et al., 2006). After 1 h a second pulse of the laser was applied and then brains were examined 1 h later.

Fluorescent in situ hybridisation and immunofluorescence

For *in situ* hybridisation probe generation, linearised plasmids containing the probe sequences for *netrin1a* (Lauderdale et al., 1997), *netrin1b* (Strähle et al.,1997) and *dcc* (Hjorth et al., 2001) were used in a dioxigenin (DIG) labelling reaction to synthesise anti-sense RNA from T7/Sp6 transcription initiation sites, as per manufacturer's instructions (Hoffman-La Roche Ltd., Basel, Switzerland). Whole mounts were incubated with an anti-digoxigenin antibody conjugated to alkaline phosphatase (1:8000; Hoffman-La Roche Ltd.). Gene expression was visualised using fast red (Hoffman-La Roche Ltd.) as the chromogenic substrate for alkaline phosphatase according to the manufacturer's instructions. Development of colour reactions was stopped by washing embryos in PBS. Embryos were then fixed for 15 h in 4% paraformaldehyde to stabilise the colour precipitate. Wholemount fluorescent *in situ* hybridisation of zebrafish embryos was followed by immunofluorescence to identify axon tracts as described previously (Hjorth and Key, 2001).

Chimeras

HuC:*kaede* donors were allowed to develop at 28.5 °C until blastula stage. The donor cells were then transplanted to the host as previously described (Kemp et al., 2009). The embryos were allowed to develop to 30 hpf before being fixed, dissected and imaged.

Image processing and analysis

Dissected brains were mounted between two coverslips to allow imaging of both sides of the same brain. Consequently, phenotype data corresponded to the number of hemi-brains. We mounted all samples in polyvinyl alcohol except for brain injected with DiI which were mounted in PBS. Image stacks were acquired using a BX61 Olympus confocal microscope with a × 40/0.75 or × 60/0.95 (oil) lens. NIH ImageJ software was used to process all confocal data sets, create confocal z projections, and perform rotation, cropping, linear contrast adjustment and channel balancing. Images presented were copy–pasted from ImageJ to Photoshop CS4 (Adobe Systems Incorporated, San Jose, California) without further modification (except for addition of scale bars). No inherent Photoshop grain-gain was used. For some images, we used the software Imaris (Bitplane, Zurich, Switzerland) to obtain a rendering of the relative positions of objects in 3-dimensional reconstructions. These images underwent non-linear modification (gamma correction) to improve final rendering without altering the information of the image itself.

Anterior commissure width

The image was rotated so that the tract of the anterior commissure was horizontal before tracing a box border around the midline of the tract. The height of the fitted box was determined using ImageJ in accordance with the image calibration. Axons that detached from the body of the tract were not included in the measurement box, guaranteeing that the dense, fascicled portion of the commissure was quantified.

Statistical analysis

Fisher's exact test was used to analyse repeats of contingency datasets generated on different days. In all cases, a two-tailed p value was obtained using GraphPad Prism version 5.00 for Windows (GraphPad Software, San Diego, California) with a 99% confidence interval. Data was pooled when the difference

between repeats was not significant. A two-tailed Fisher's exact test was used to compare between the experimental and control groups. A one-way ANOVA analysis of the data followed by a Tukey post-test was used to compare the differences between grouped data. Fisher's exact test was used to determine whether the effect of sub-threshold double knock downs of both *ntn1a* and *dcc* was greater than the additive effects of each single gene knock down alone. Greater than additive effects indicate genetic interactions are occurring as a result of genes acting in either the same biochemical or genetic pathway (Guarente, 1993; Cordell, 2002). The observed penetrance of *ntn1a* and *dcc* double knock downs was compared to the additive penetrance of single knock downs (*ntn1a*+*dcc*) minus the penetrance of the control group (which was normalised to the frequency of the sample size of the combined single *ntn1a* and *dcc* knock downs). The subtraction of the control group penetrance was necessary since addition of two single knock downs duplicates, and hence overestimates, the effect of background levels of the phenotype.

Results

Dcc loss-of-function generates an ectopic axon bundle in the diencephalon

In order to begin to understand how chemoattractant axon guidance molecules contribute to formation of the embryonic axon scaffold we have examined the role of Dcc and its Netrin1 ligands during early embryonic forebrain development in zebrafish. Immunostaining for growing axons in wholemounts of embryonic zebrafish brain enabled us to uniquely observe aberrant axon growth and guidance within the context of the entire axon scaffold and during the earliest stages of tract formation in the vertebrate brain. The loss of function of *dcc* produced by previously characterised translational blocking antisense morpholinos (MOs; Suli et al., 2006; Kastenhuber et al., 2009; Lim et al., 2011) did not affect the establishment of the major axon tracts or their gross patterning within the initial scaffold (Fig. 2A and C). Lateral views of the embryonic brain revealed that the tract of the post-optic commissure continued to develop and course along the ventrolateral surface of the brain following knock down of *dcc* (Fig. 2A and C). Similarly, the major dorsoventrally projecting axon tracts (Fig. 1) including the supraoptic tract, dorsoventral diencephalic tract and tract of the posterior commissure also formed normally in *dcc* loss-of-function embryos (Fig. 2A and C). While axon tracts emerged in a normal spatiotemporal pattern, loss of *dcc* selectively led to the development of mis-projecting axons coursing from the caudal telencephalon into the dorsal diencephalon. These ectopic axons invaded the normally axon-free neuroepithelium in the dorsal diencephalon (thin arrows, Fig. 2C and D). These axons typically formed a discrete bundle that followed a curved route, beginning from the dorsocaudal margin of the telencephalic cluster of neurons and extending caudally and then ventrally towards the tract of the post-optic commissure (thin arrows, Fig. 2C). These ectopic axons merge with the first tract they meet during their trajectory; it can be either the pioneering axons of the tract of the habenular commissure which are beginning to extend dorsally from the ventral diencephalon at 30 hpf (Figs. 1 and 2A), or the tract of the postoptic commissure (large arrow, Fig. 2E), or the dorsoventral diencephalic tract (Fig. 2C). From a dorsal view, no ectopic axons were observed in controls (Fig. 2B). In contrast, in *dcc* knock down embryos ectopic axons typically formed a discrete bundle exiting the causal telencephalon (arrows, Fig. 2D). Occasionally these axons appeared defasciculated (thin arrows, Fig. 2F), but in most cases they formed a single tight bundle (thin arrows, Fig. 2D and F).

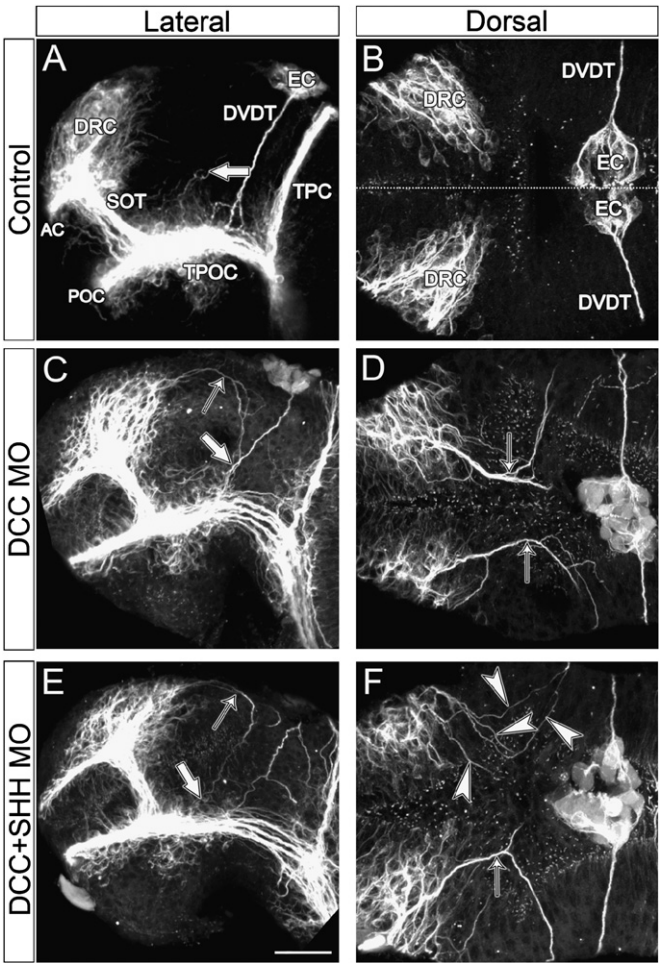

Fig. 2. *dcc loss-of-function generates an ectopic axon bundle in the diencephalon*. All images are confocal projections of zebrafish whole-mounted brains at 30 hpf immunolabelled for expression of acetylated α-tubulin. Anterior is left in all images. (A) The axon tracts are displayed according to Fig. 1. Note the absence of axons in the diencephalic territory between the DVDT and DRC–SOT except for a few pioneers of the future THC (large arrow). (B) Note the absence of any axon tract in the diencephalic space separating the DRC from the EC. The dotted line represents the midline. (C) Axons emerging from the posterior edge of the DRC and extending into the diencephalon are indicated by the thin arrows. These axons typically follow a curved route through the diencephalon down to the TPOC, meeting with the pioneers of the THC extending dorsally or the DVDT (large arrow). (D) The ectopic axons clearly extend from the caudal margins of the DRC into the dorsal diencephalon. Most axons are tightly bundled at the exit of the telencephalic cluster. (E) Co-knockdown of *shh* and *dcc* did not rescue the phenotype of these ectopic diencephalic axons nor did it alter their route ventrally (arrow) since they still connect with the TPOC (large arrow). (F) While the left side shows a typical tightly-fasciculated bundle of ectopic axons (arrow), the right side of this embryo exhibits axons wandering individually in the dorsal diencephalon (arrowheads). These individual axons appear to be still following a stereotypical route as in the contralateral side of the brain. Scale bar=35 μm (A, C, E), 20 μm (B, D, F).

The ectopic axons initially seemed to point towards the mid-telencephalic territory where *Sonic hedgehog* is expressed and is known to be an important organiser of thalamic differentiation (Scholpp et al., 2006) as well as a potential chemoattractant (Charron et al., 2003). In this context, we co-injected 1 ng of *shh* MO with *dcc* MO to test whether loss of Shh could rescue the ectopic axon phenotype. However, knock down of *shh* did not rescue the phenotype (Fig. 2E and F) indicating that other cues are directing the growth of these ectopic axons. The *shh* MO was particularly potent as increasing the dosage triggered gross defects in the embryos as previously reported with loss of *shh* (Prykhozhij, 2010).

We quantified the penetrance of this ectopic axon bundle phenotype at different doses of MO by counting the occurrence of ectopic fibres in the dorsal diencephalic area (Fig. 3A). Interestingly, 9% of control brains (25 out of 275) exhibited some axons invading the diencephalic region of interest. This result suggested to us that natural stochastic variations in the expression of *dcc* may lead to the misguidance of ectopic axons caudally from the dorsorostral cluster. If this was true we would expect to see increasing penetrance of the phenotype with progressive loss of *dcc*. Our dose-response analysis confirmed that increasing the amount of *dcc* MO injected did result in a selective increase in the presence of ectopic axons exiting caudally from the dorsorostral cluster. The control penetrance was significantly exceeded with doses of *dcc* MO as low as 0.25 ng ($P=0.0022$; $P<0.0001$ for higher doses). A plateau of around 80% was reached at 1 ng MO while the maximum penetrance observed was 93% using 5 ng of MO. Because of the high penetrance of this phenotype, and the consistency and the bilateral symmetry of the axon trajectories in the knock down embryos we have referred to these axons as forming the "ectopic diencephalic axon bundle" (EDAB).

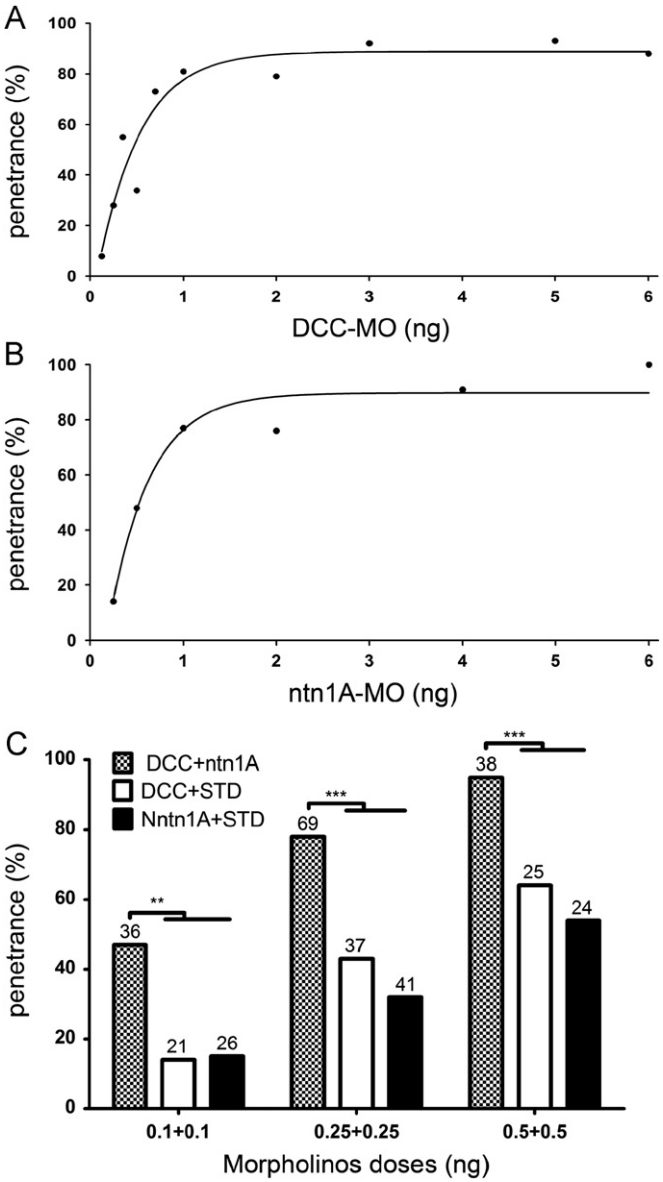

Fig. 3. *dcc and ntn1a loss of function produce the same phenotype with similar penetrance*. The graphs represent the percentage of brains exhibiting an ectopic diencephalic axon bundle (EDAB) for each dose of MO (in ng). The number of samples (n) examined as well as the P value in the Fisher exact test comparing each dose to controls are presented below. (A) Dose–response curve for *dcc* MO. (0.125 ng, $n=24$, $P=1$; 0.25 ng, $n=32$ $P=0.0022$; 0.5 ng, $n=50$; 0.7 ng, $n=24$; 1 ng, $n=42$; 2 ng, $n=38$; 3 ng, $n=63$; 5 ng, $n=40$; 6 ng, $n=16$; $P<0.0001$ for all doses equal or above 0.5 ng). (B) Dose–response curve for *ntn1a* MO. (0.25 ng, $n=43$, $P=0.2455$; 0.5 ng, $n=102$; 1 ng, $n=43$; 2 ng, $n=33$; 4 ng, $n=11$; 6 ng $n=16$. $P<0.0001$ for all doses equal or above 0.5 ng). (C) Penetrance observed after injection of different combinations of *dcc*, *ntn1a* and STD MO. The levels of statistical difference determined via Fisher's exact test are represented by asterisks. Numbers on top of each bar represent the number of hemi-brains investigated. The penetrance in *dcc*+STD and *ntn1a*+STD were not statistically different while all doses of the *dcc*+*ntn1a* combinations show a significant difference with their control counterparts.

These results indicate that *dcc* appears to be selectively involved in the guidance of a subpopulation of axons arising from the dorsorostral cluster in the telencephalon. This phenotype is consistent with our earlier observations that *dcc* is initially expressed by a small subpopulation of neurons residing in the caudal portion of the dorsorostral cluster (Hjorth et al., 2001) and confirmed here (Supplementary Fig. 1). In the absence of *dcc*, it appears that some telencephalic axons reproducibly exit the caudal margins of the dorsorostral cluster of neurons to form a bundle that we refer to as the EDAB. This bundle of axons courses ventrally along a curved trajectory towards the tract of the post-optic commissure. This is the first time that an axon bundle has been reported to be formed *de novo* in the embryonic forebrain through manipulation of the level of expression of a single axon guidance receptor.

ntn1a interacts with dcc to inhibit development of the ectopic diencephalic axon bundle

In order to determine whether the development of the EDAB is normally prevented by interaction of Dcc with its Netrin1 ligands, we next investigated the effect of knocking down either of the two paralogues of netrin1 in zebrafish: *ntn1a* or *ntn1b* (MacDonald et al., 1997; Strähle et al., 1997; Lauderdale et al., 1997). Knocking down *ntn1a* using 0.5 ng or more of MO (as described previously: Suli et al., 2006; Kastenhuber et al., 2009; Lim et al., 2011) led to an axon guidance phenotype that was indistinguishable from that observed with *dcc* loss of function. In the absence of *ntn1a*, ectopic axons were again observed to exit the dorsocaudal margin of the dorsorostral nucleus of the telencephalon and grow into the ipsilateral or contralateral dorsal diencephalon before turning and growing ventrally to form the EDAB (Figs. 3B and 4A and B). While the dose–response curve for *ntn1a* knock down (Fig. 3B) was similar to that obtained for *dcc* loss-of-function (Fig. 3A), 0.5 ng of *ntn1a* MO rather than 0.25 ng of *dcc* MO was required to significantly elicit a phenotype ($P<0.0001$). In marked contrast, knocking down *ntn1b* (Fig. 4C and D) failed to produce the EDAB phenotype seen following loss of function of either *dcc* (Fig. 2C and D) or *ntn1a* (Fig. 4A and B). Embryos injected with up to 4 ng of *ntn1b* MO did not show signs of the EDAB ($n=38$). Despite the absence of the EDAB phenotype, the *ntn1b* MO (as previously described: Suli et al., 2006; Kastenhuber et al., 2009) was active since it consistently and very selectively caused mistargeting of a subpopulation of anterior commissural axons into the neuroepithelium lying ventral to this commissure (thin arrows, Fig. 4C; compare with Fig. 4A). Aberrant projecting anterior commissural axons were not observed in either the *dcc* or *ntn1a* knock down animals.

Taken together, these results suggest that *ntn1a* and *dcc* are acting in the same genetic pathway to modulate axon guidance and restrict the formation of the EDAB during normal development. When expression of either the *dcc* receptor or its *ntn1a* ligand was reduced, a subpopulation of dorsorostral cluster

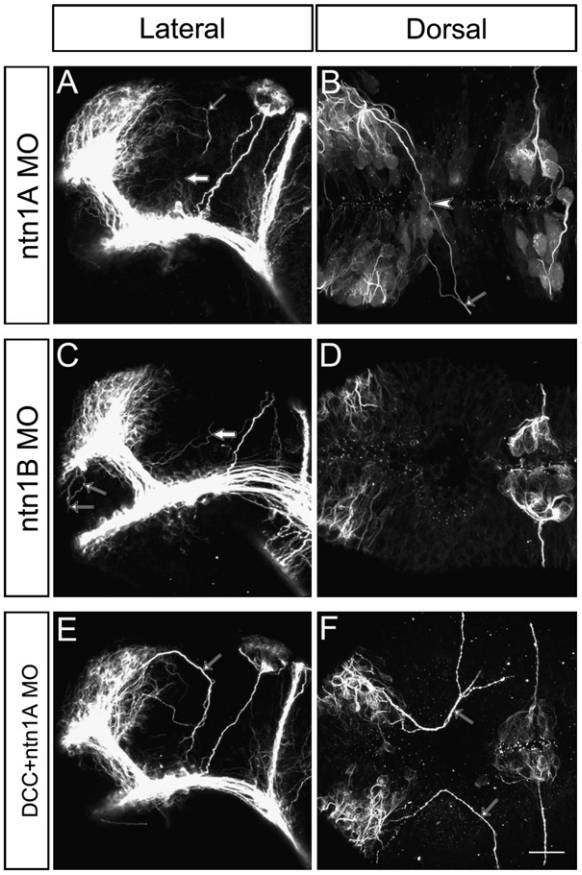

Fig. 4. *Knocking down ntn1a, but not ntn1b, reproduces the dcc loss of function phenotype.* All images are confocal projections of zebrafish whole-mounted brains at 30 hpf immunolabelled for expression of acetylated α-tubulin. (A) Ectopic axons emerge from the caudal edge of the DRC (thin arrow). The large arrow indicates THC pioneer axons that extend from the ventral diencephalon. (B) Ectopic axons emerge caudally from the DRC. In this example, the tract emerging from the right side of the telencephalon crosses the midline (arrowhead) and invades the contralateral diencephalon before joining the contralateral ectopic axons and continuing the stereotypical curved route to the ventral part of the diencephalon (thin arrow). (C) No ectopic axons are visible in the diencephalic territory caudal to the DRC except for the ventrally located pioneers of the THC (large arrow). Note the axons ventral to the AC that seem to detach themselves from the bulk of the commissure (thin arrows). (D) No ectopic axons are observed in the dorsal diencephalon. (E) The ectopic axon tract follows a stereotypical course through the diencephalon (thin arrow). (F) Ectopic axons (arrows) do not always cross the midline. Scale bars = 40 μm (A, C, E), 20 μm (B, D, F).

neurons appeared to extend caudally and inappropriately create the EDAB. Interestingly, while the netrin1 paralogues, *ntn1a* and *ntn1b*, have distinct axon guidance phenotypes, they are both active in axons which appear to arise from the dorsorostral cluster of neurons in the telencephalon.

In order to verify that *ntn1a* and *dcc* were genetically interacting, we co-injected sub-threshold levels of MO that by themselves failed to produce a significant phenotype. When 0.1 ng of *ntn1a* and *dcc* MO were co-injected there was a significant increase ($P=0.0016$) in the penetrance of the EDAB phenotype compared with co-injection of either the *dcc* or *ntn1a* MO and 0.1 ng of control MO (Fig. 3C). Thus, the simultaneous sub-threshold knock downs of *dcc* and *ntn1a* suggested that these two genes were genetically interacting to regulate the EDAB phenotype. Since this increase in penetrance was greater than the additive effect of the combined single knock downs ($P<0.0001$), it indicates that these genes are indeed genetically interacting and that they are acting in the same pathway (Guarente, 1993). We also observed a significantly greater penetrance in double knock downs for doses below 1 ng as compared to their single knock down counterparts ($P<0.0001$ for $0.25+0.25$ ng; $p=0.0001$ for $0.5+0.5$ ng). However, at 1 ng or above, while the penetrance of double and single knock downs was not different ($P=0.0675$ for $1+1$ ng), the phenotype was more severe in the double knock downs. In these latter animals the EDAB was typically thicker and more prominent (thin arrows, Fig. 4E and F). This increased severity in double knock downs provided further evidence that *dcc* and *ntn1a* are acting synergistically to regulate development of the EDAB. The observations that loss of function of either *dcc* or *ntn1a* produces the same phenotype, that there is a greater than additive effect of double sub-threshold knock downs of *dcc* and *ntn1a* and that there is an enhanced phenotype of double knock downs have confirmed the specificity of the MO knock down approach as well as demonstrated that *dcc* and *ntn1a* function in the same signalling pathway.

In all *dcc* and *ntn1a* MO knock downs, we observed 528 EDAB. Out of these, 267 extended from the telencephalon ventrally to the TPOC via a stereotypical curved route as shown in Figs. 2C and E and 4E. Another 217 exhibited a similar route but did not fully extend ventrally to the TPOC. In 28 cases, the ectopic fibres crossed the midline (Fig. 4B), and in 16 cases some axons crossed the midline while some extended ventrally. Taken together, this shows that 92% of the EDAB extend ventrally in a stereotypical route through the diencephalon while 8% of the EDAB cross the dorsal midline.

The EDAB is distinct from the stria medullaris

Although the idea that loss of interactions between Dcc and Ntn1a was responsible for the creation of a novel axon bundle is strongly supported by the data, it was possible that manipulating the levels of these molecules was instead affecting heterochrony or the timing of axon tract formation in the zebrafish brain. That is, perhaps an axon tract that typically forms later in development in the position of the EDAB was prematurely arising following loss of either *dcc* or *ntn1a*. The stria medullaris is the only axon tract that develops in the vicinity of the EDAB in wild-type embryos (Wilson et al., 1990; Hendricks and Jesuthasan, 2007). Immunostaining for growing axons in wild-type embryos revealed that axons forming this tract begin to exit the dorsocaudal margin of the telencephalon at 36 hpf and project caudally across the mid-region of the diencephalon (chevron, Fig. 5A). At this age, both the caudally-oriented stria medullaris and the dorsally-projecting tract of the habenular commissure (arrow, Fig. 5A) consist of only a few pioneering axons. However, within a further 12 h of development both tracts are well established and the stria medullaris has merged with the tract of the habenular commissure, which now crosses the dorsal midline (large arrow, Fig. 5B). Typically no ectopic axons were visible in the dorsal diencephalon in the region where we observed the EDAB in *dcc* and *ntn1a* loss of function brains.

In order to determine the relationship between the EDAB and both the stria medullaris and tract of the habenular commissure, we compared control and knock down brains at 48 hpf when the two latter tracts are clearly distinguishable in the forebrain. In dorsal and lateral views of the brains lacking both *dcc* and *ntn1a* (Fig. 5C and D) we were able to observe the EDAB (thin arrow, Fig. 5C and D) as separate and distinct from the stria medullaris (chevron, Fig. 5C and D). While both merged with the tract of the habenular commissure (large arrow, Fig.5C and D), the EDAB followed a caudoventral trajectory as opposed to the caudodorsal orientation of the stria medullaris. The EDAB was not only distinguished from the stria medullaris by its dorsal position in the diencephalon but also by having axons that occasionally cross the midline (arrowhead, Fig. 5C). These results have now shown that loss of *dcc-ntn1a* interactions did not produce heterochronic changes in the

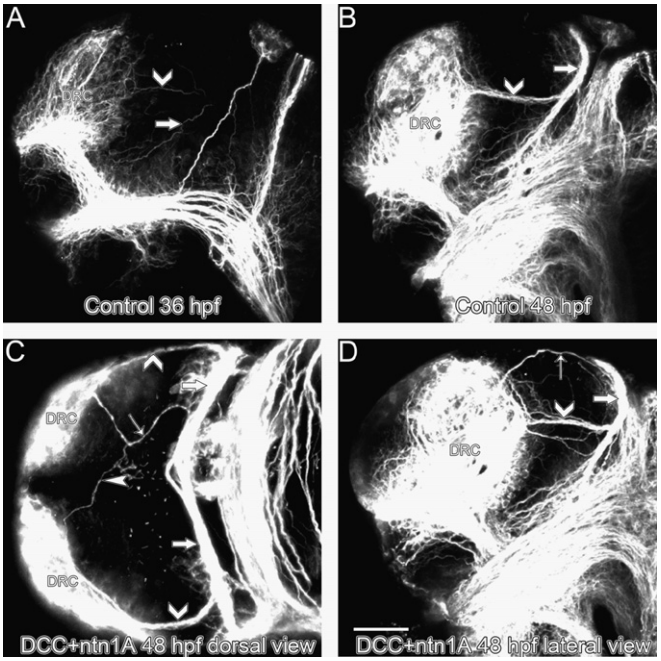

Fig. 5. *EDAB is distinct from the stria medullaris*. All images are confocal projections of zebrafish whole-mounted brains immunolabelled for expression of acetylated α-tubulin. (A), (B), (D) Lateral view (anterior is left, dorsal is up). (C) Dorsal view (anterior is left). (A) At 36 hpf, two new axon tracts extend into the diencephalon: the tract of the habenular commissure (large arrow) and the pioneer axons of the stria medullaris (chevron arrow). (B) At 48 hpf, the stria medullaris (chevron arrow) and the tract of the habenular commissure (large arrow) have both enlarged considerably and have fused together to project to the habenula in the dorsal diencephalon. (C) Dorsal view of a 48 hpf *dcc+ntn1a* MO injected brain exhibiting the typical ectopic diencephalic axon tract in the dorsal diencephalon (thin arrow). Note that the left-side ectopic tract crosses the midline (arrowhead) before merging with its contralateral counterpart. The ectopic tract that remained ipsilateral merged with the THC (large arrow). Chevron arrows indicate the stria medullaris on both sides. (D) Lateral view of a 48 hpf *dcc+ntn1a* MO injected brain. Note the dorsal ectopic tract (thin arrow) that is distinct from the stria medullaris (chevron arrow) and fusing into the THC (large arrow). Scale bars = 40 μm (A, B, D), 30 μm (C).

development of the axon scaffold but instead it clearly led to the *de novo* formation of a novel axon bundle coursing from the caudal telencephalon into the dorsal diencephalon.

The EDAB originates from a caudal subset of neurons in the dorsorostral cluster of the telencephalon that normally project into the anterior commissure

Since *dcc* is selectively expressed in the caudal portion of the dorsorostral cluster of neurons in the telencephalon (Hjorth et al., 2001, Supplementary Fig. 1A) we reasoned that the ectopic axons forming the EDAB were arising from this same region as suggested by immunostaining of a *ntn1a* MO knock down brain co-labelled for *dcc* mRNA (Supplementary Fig. 1B). In order to determine the neuroanatomical origin of the EDAB, we used several complementary approaches. First, we took advantage of *HuC*:*kaede* fish (Sato et al., 2006) expressing the green fluorescent kaede protein in post-mitotic neurons under the control of the *HuC* promoter. When this protein is irradiated with ultraviolet light its fluorescence shifts to red wavelengths which allows the trajectory of small subpopulations of neurons to be traced when they are selectively irradiated with ultraviolet light. We injected 3 ng of the *dcc* MO into *HuC*:*kaede* embryos and at 24 hpf examined live animals for the presence of the EDAB. We failed to photoconvert any EDAB axons from green to red fluorescence (arrowheads, Fig. 6A) when the anterior half of the dorsorostral cluster of neurons was irradiated with ultraviolet light. The irradiation of the dorsorostral cluster was successful since photoconverted red axons were found projecting into the supraoptic tract in these preparations (arrow, Fig. 6A). Only when the posterior half of the dorsorostral cluster was irradiated were EDAB axons photoconverted from green to red (arrowheads, Fig. 6B). These results were consistent with the EDAB arising from *dcc* expressing neurons in the caudal dorsorostral cluster. Interestingly, we also observed that the posterior and not the anterior half of the dorsorostral cluster gave rise to axons that formed the anterior commissure in these *dcc* knock down brains (chevron, Fig. 6B).

The above results revealed that the neurons forming the EDAB were most likely localised in the caudal half of the dorsorostral cluster and that this region of the nucleus normally projected axons into the anterior commissure. However, when we examined lateral views of brains we found that the confocal laser irradiation of the dorsorostral cluster coursed through the depth of the dorsal–ventral axis of the brain (dotted line, Fig. 6C and D) causing unwanted ventral neurons to be photoconverted. Thus, it was possible that axons from these ventral-labelled neurons could have projected via the supraoptic tract (arrows, Fig. 6C and D) into both the anterior commissure (chevrons, Fig. 6C and D) and EDAB (arrowhead, Fig. 6D). We next created chimeric animals consisting of *HuC*:*kaede* transgenic donor cells in wild-type host brains in an attempt to obtain mosaic animals with green donor cells within the dorsorostral cluster. We managed to obtain four chimeric animals hosting *kaede* donor cells in the dorsorostral cluster. The control *kaede*-expressing neurons (arrows, Fig. 6E and F) projected their axons into the anterior commissure (arrowheads, Fig. 6E and F) and/or supraoptic tract (thin arrow, Fig. 6F) in four animals investigated, confirming our results above using photoconversion.

To further characterise the origin of the EDAB and anterior commissure we next used DiI microiontophoresis into fixed brains of *HuC*:*kaede* animals. When DiI was applied to the EDAB in *dcc* knock down brains we could clearly follow axons from the injection site (thick arrow, Fig. 6G) both retrogradely to their neurons of origin in the caudal portion of the dorsorostral cluster (arrowhead, Fig. 6G) and anterogradely towards their growing end (thin arrow, Fig. 6G). The retrogradely decorated neurons were localised in the posterior half of the dorsorostral cluster and consisted of only a few superficially localised perikarya (arrowheads, Fig. 6H and J). Using DiI retrograde tracing we were able to identify a maximum number of three neuronal cell bodies with axons in the EDAB at 24 hpf. To further ascertain that neurons localised in the caudal part of the dorsocaudal cluster project predominantly into the anterior commissure, we applied DiI directly into the anterior commissure (large arrow, Fig. 6K and K′). This technique led to selective anterograde labelling of neurons localised in the caudal half of the dorsorostral cluster (arrowhead, Fig. 6K and K′). Next, when DiI was then applied to the caudal half of the dorsorostral cluster (large arrow, Fig. 6L and L′), axons in the anterior commissure were retrogradely labelled (arrowhead, Fig. 6L and L′).

Taken together, these tracing experiments have demonstrated that neurons located in the caudal portion of the dorsorostral cluster normally project the majority of their axons into the anterior commissure. When we perturb *dcc-ntn1a* signalling, some of these neurons failed to project rostrally and extended their axons caudally and inappropriately into virgin dorsal diencephalic neuroepithelium to form the EDAB.

The EDAB projects mainly to the ventro-rostral cluster via the superficial diencephalic neuroepithelium

In order to more clearly characterise the ventral target of the EDAB, we injected DiI into the caudal telencephalon around

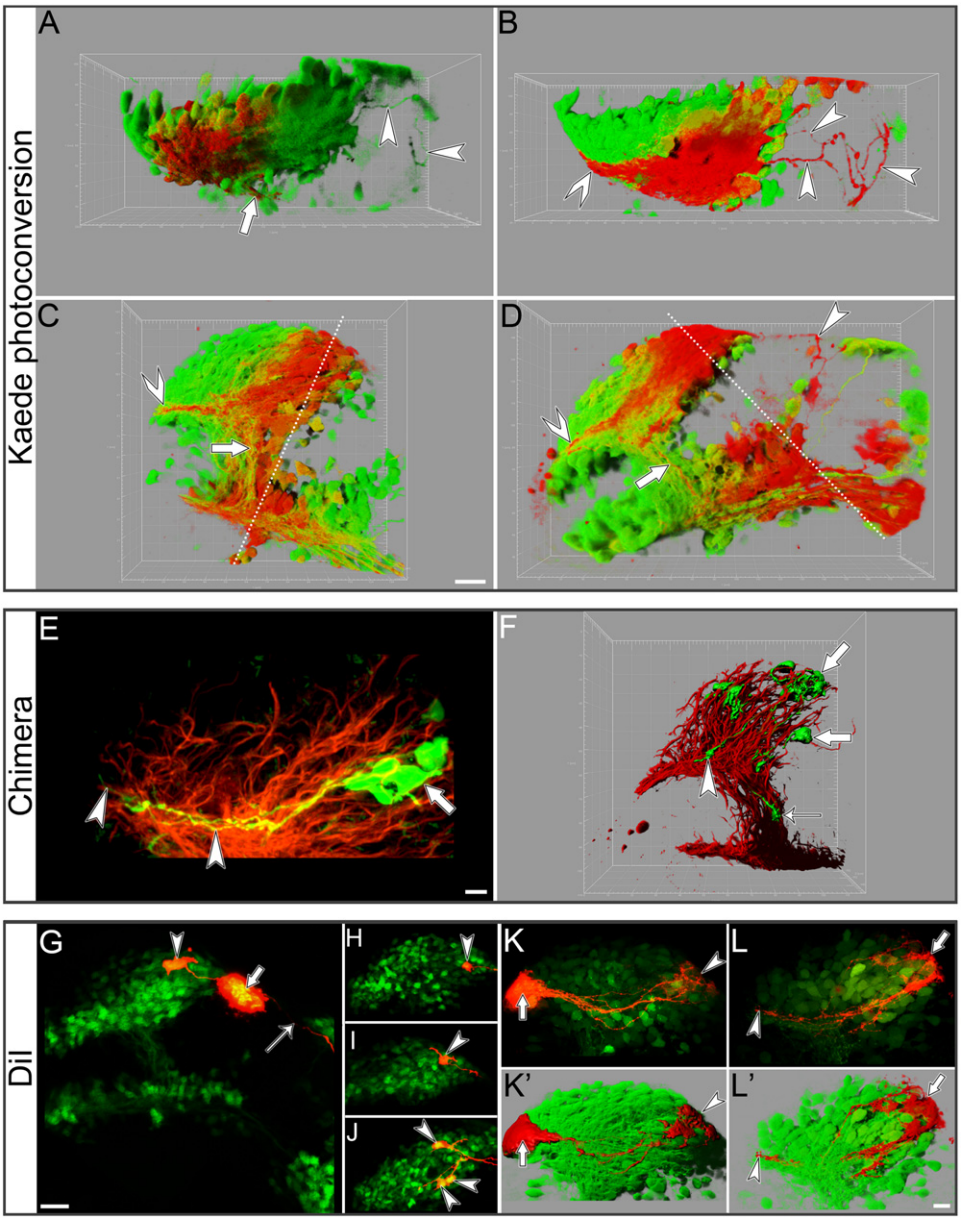

Fig. 6. *EDAB originates from a subset of neurons in the caudal portion of the DRC that normally project into the anterior commissure*. Axon tracing using kaede photoconversion (A–D), chimeras (E–F) and DiI (G–L′). All images are confocal image stacks processed with Imaris software. The resulting representation are either a simple maximum intensity projection under orthogonal perspective along the *Z* axis (E–K), perspective views of shadow projection rendering of the stacks (A–D, K′, L′) or a mix of shadow projection rendering and volume rendering (F). (A) Dorsal view of the DRC in a *dcc* knock down embryo at 30 hpf. When the anterior portion of the DRC was photoconverted (red), the EDAB remained green (arrowheads) while red photoconverted axons exited via the SOT (large arrow). (B) Dorsal view of the DRC in a *dcc* knock down embryo at 30 hpf. When the posterior portion of the DRC was photoconverted (red) the EDAB was red (arrowheads). Note also the large number of photoconverted axons extending towards the anterior commissure (chevron). (C) Lateral view of a control brain at 30 hpf. The dotted line indicates the path of the photoconverting laser through the DRC and the underlying VRC. When the posterior portion of the DRC is photoconverted (red) in a control brain, both the anterior commissure (chevron arrow) and SOT (large arrow) are labelled in red. (D) Lateral view of a *dcc* knock down embryo at 30 hpf. The dotted line represents the path of the photoconverting laser through the DRC and the caudal VRC and TPOC. The EDAB (arrowhead), anterior commissure axons (chevron arrow) and SOT axons (large arrow) are all labelled in red. (E) Lateral view of the DRC in a wild-type host chimeric animal immunolabelled for expression of acetylated α-tubulin (red) showing the axon trajectory of donor neurons expressing kaede from the caudal edge of the DRC (large arrows) into the anterior commissure (arrowheads). (F) Lateral view of the forebrain of a wild-type host chimeric animal immunolabelled for expression of actetylated α-tubulin (red) showing growth cones of kaede-expressing donor cells (large arrow) in the anterior commissure tract (arrowhead) and the SOT (thin arrow), representing the two routes used by axons originating from the caudal half of the DRC. (G) Lateral view of the forebrain of a *dcc* knock down embryo showing the site of microiontophoretic deposit of DiI in the route of the EDAB (large arrow). The EDAB axon is anterogradely labelled (thin arrow). Retrograde labelling reveals the cell body of the neuron located at the dorsocaudal end of the DRC (arrowhead). (H)–(J) Lateral views showing the localisation of the cell bodies giving rise to the EDAB in the caudal half of the DRC (arrowheads) after retrograde DiI labelling of the EDAB. (K)–(K)′ Lateral view of the DRC in a control embryo after injection of DiI in the anterior commissure (large arrow). Axons are retrogradely labelling the cell bodies located at the dorsocaudal end of the DRC (arrowhead). (L)–(L)′ Lateral view of the DRC in a control embryo after injection of the DiI at the dorsocaudal end of the DRC (large arrow) labelling axons anterogradely in the tract of the anterior commissure. These axons enter the anterior commissure after passing the point where the SOT bifurcates from the tract. Scale bars = 15 μm (A–D), 5 μm (E), 10 μm (F), 20 μm (G), 25 μm (H–J), 10 μm (K–L′).

30 hpf in *HuC*:*kaede* fish (Fig. 7). As expected, some axons in both the anterior commissure (arrowheads, Fig. 7) and supraoptic tract (large arrow, Fig. 7) as well as in the EDAB were labelled by the dye. The DiI labelled axons in the EDAB could be traced to the caudal portion of the ventrorostral cluster in both *dcc* and *ntn1a* knock downs (thin arrows, Fig. 7A and B). This group of cells gives rise to the axons of the tract of the habenular commissure which sometimes fasciculates with the EDAB. We could clearly establish that the EDAB was coursing in the superficial-most layer of the columnar neuroepithelium immediately adjacent to the ventricle. In this respect the trajectory of the EDAB resembles that of the dorsoventral diencephalic tract, as observed in 3-dimensional renditions (Supplementary movies 1–4).

Roles of dcc and netrin1 in the development of the anterior commissure

Since loss of either *dcc* or *ntn1a* caused a subpopulation of dorsorostral cluster axons to project caudally rather than anteriorly towards the anterior commissure, we predicted that there would be abnormalities in the development of this latter tract. Indeed, when we examined frontal plane images of the rostral surface of 30 hpf brains we observed a clear reduction in the thickness of the anterior commissure in *dcc* (arrowhead, Fig. 8C) and *ntn1a* (not shown) knock downs compared to controls (Fig 8A). Interestingly, knocking down *ntn1b* did not appear to reduce the bulk of the anterior commissure, but instead led to the presence of aberrant axons wandering into the neuroepithelium ventral to the anterior commissure (arrow, Fig. 8E). These aberrant axons entered the ventral neuroepithelium from the lateral edges of the tract of the anterior commissure (arrowheads, Fig. 8E). We measured the thickness the anterior commissure at 30 hpf and compared controls to *dcc*, *ntn1a* and *ntn1b* knock downs (Fig. 9). Loss of function of either *dcc* or *ntn1a*, but not *ntn1b*, led to a significant reduction of the anterior commissure compared to controls. This reduced anterior commissure phenotype appeared to be restricted to a defined temporal window since by 48 hpf, the anterior commissures in *dcc* and *ntn1a* (Fig. 8D) knock downs were indistinguishable from controls (Fig. 8B). In contrast, the aberrant axons coursing ventral to the anterior commissure in *ntn1b* knock down brains persisted at 48 hpf (arrows,

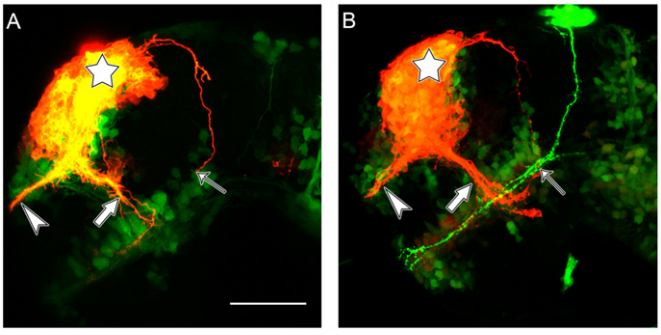

Fig. 7. *Tracing the EDAB to the ventrorostral diencephalic cluster*. (A) *HuC*:*kaede* brain. (B) *HuC*:*kaede*/*Foxd3*:*GFP* brain. DiI labelling is represented in red and the kaede/GFP fluorescence in green. The star indicates the site of DiI injection, the arrowhead indicates the anterior commissure, the large arrow is the supraoptic tract and the thin arrow points at the identifiable end of the EDAB. In (B) the DVDT trajectory is clearly depicted by GFP fluorescence in green. Scale bar = 50 μm.

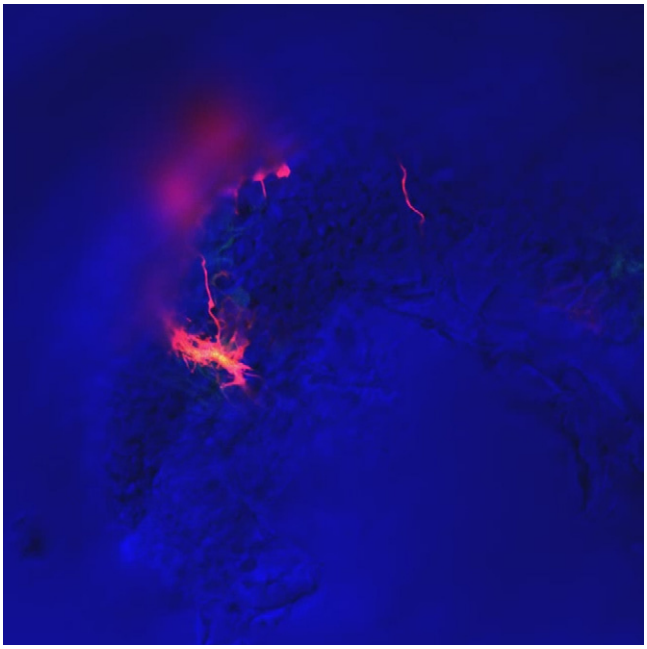

Movie S2. Supplementary movie 2. Confocal stack used to produce movie 1 and Fig. 7**(A)**. Note that the EDAB (in red) is coursing in the superficial neuroepithelium (seen in transmitted light in the blue channel) like the DVDT (in green) before reaching the VRC. http://dx.doi.org/10.1016/j.ydbio.2012.04.032.

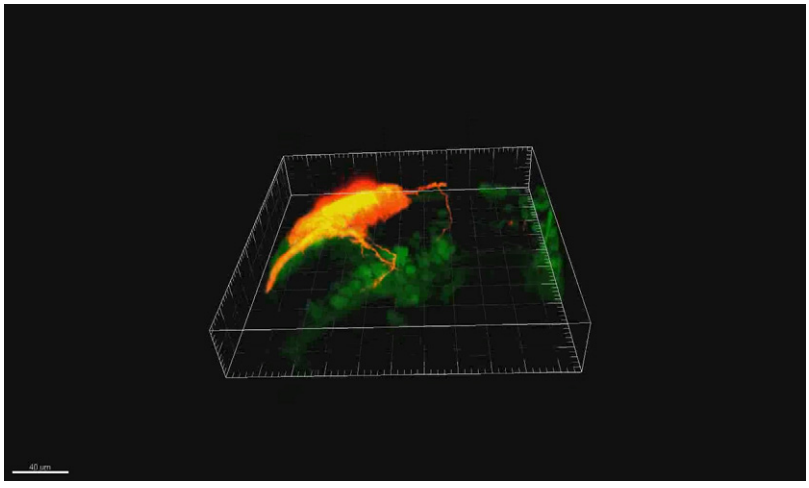

Movie S1. Supplementary movie 1. 3D reconstruction of the *dcc* knock down brain shown in Fig. 7**(A)**. Note the curved trajectory of the EDAB (in red) following the curvature of the neuroepithelium overlying the third ventricle. http://dx.doi.org/10.1016/j.ydbio.2012.04.032.

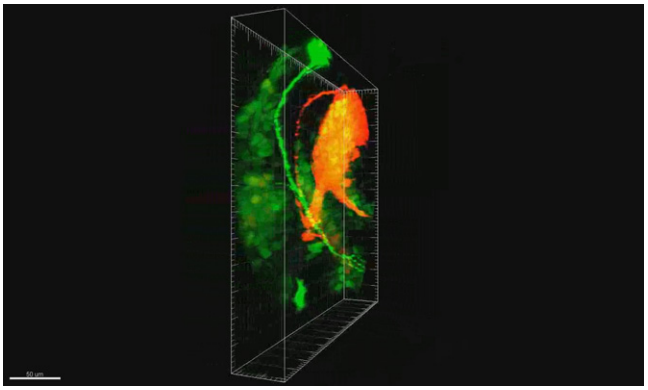

Movie S3. Supplementary movie 3. 3D reconstruction of the *ntn1a* knock down brain shown in Fig. 7(**B**). Note the curved trajectory of the EDAB (in red) following the curvature of the neuroepithelium overlying the ventricle. Compare it to the course of the DVDT strongly labelled in green because of the expression of GFP under the *foxd3* promoter in the epiphysis. http://dx.doi.org/10.1016/j.ydbio.2012.04.032.

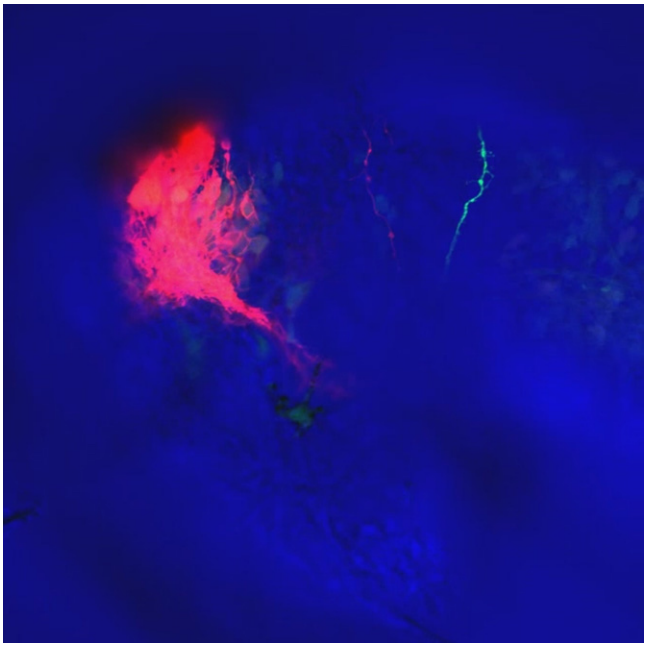

Movie S4. Supplementary movie 4. Confocal stack used to produce Supplementary movie 3 and Fig. 7(**B**). Compare the trajectory of the EDAB (in red) with the DVDT (in green) and their progression in respect to the neuroepithelium (in the blue channel as transmitted light) and the ventricle. http://dx.doi.org/10.1016/j.ydbio.2012.04.032.

Fig. 8F). As at 30 hpf, these aberrant axons mainly entered the ventral neuroepithelium from the lateral margins of the tract of the anterior commissure (arrowheads, Fig. 8F).

Together, these results indicate that *dcc* and *ntn1a* were interacting to both generate the EDAB phenotype as well as simultaneously reduce the thickness of the anterior commissure, albeit transiently. Contrary to *ntn1a*, *ntn1b* seems to be acting independently of *dcc* to restrict axons to within the anterior commissure.

Netrin1 paralogues have different expression patterns in the anterior forebrain

We reasoned that the different functions of the netrin paralogues in development of the anterior commissure could be explained by differences in the spatial expression patterns of these molecules. Unfortunately, previous studies have not clearly reported the relationships of *ntn1a* and *ntn1b* expression to the trajectories of commissural tracts as they cross the midline (Lauderdale et al., 1997; Park et al., 2005). We have found here that both *ntn1a* and *ntn1b* are expressed in an overlapping triangular wedge of neuroepithelium located in the midline within the telencephalon (dotted triangles, Fig. 9A and B). The *ntn1b* wedge is much smaller and appears contained within the *ntn1a* domain in the midline. *ntn1b*, but not *ntn1a*, has a lateral domain of expression that extends into the diencephalon (dotted ovals, Fig. 9B). Three dimensional reconstructions of the confocal scans depict the spatial relationship of the anterior and post-optic commissures to the expression domains of the netrin1 paralogues (Fig. 9C and H; Supplementary movies 5 and 6). Frontal views reveal that the axons of the anterior commissure are clearly separated from the lateral domain of *ntn1b* (double arrows, Fig. 9D). Viewed dorsally and laterally, the *ntn1a* and *ntn1b* domains create a rostral strip of netrin1 expression that defines the anterior surface of the brain (Fig. 9E and H). The anterior

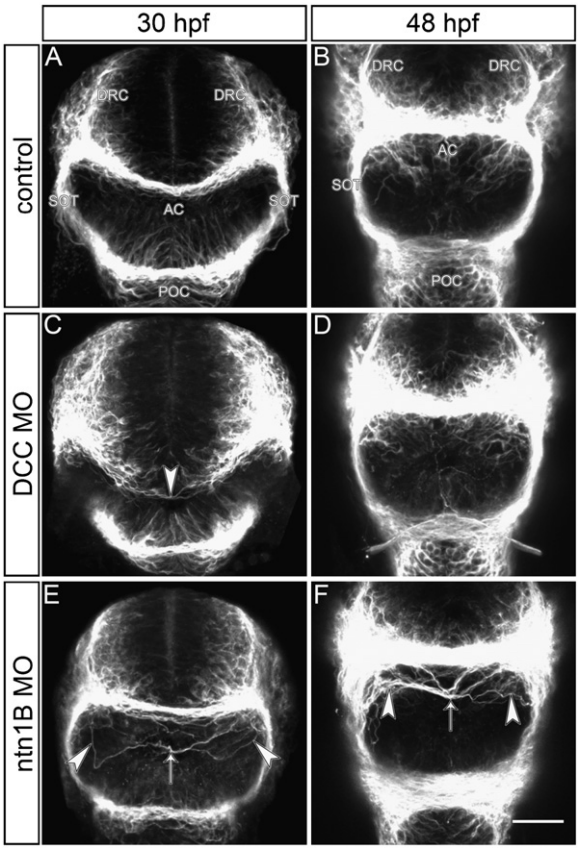

Fig. 8. *dcc/ntn1a and ntn1b loss of function produce very distinct phenotypes in the anterior commissure*. All images are confocal projections from a frontal view on the commissural plate immunolabelled for expression of acetylated α-tubulin. Dorsal is up. Upper horizontal tract is the anterior commissure; lower horizontal tract is the post-optic commissure. Vertical tracts occasionally visible are the SOTs. (A) Control brain at 30 hpf. (B) Control brain at 48 hpf. Note how both tracts have thickened. (C) *dcc* knock down embryo at 30 hpf. Note the reduction of AC at the midline (arrowhead) but not the POC. (D) *dcc* knock down embryo at 48 hpf. The reduction of the AC is no longer detectable when compared to 30 hpf. E. *ntn1b* knock down embryo at 30 hpf. Arrowheads show the lateral detachment of the ectopic axons (arrowheads) invading the inter-commissural space ventral to the anterior commissure (thin arrow). The bulk of the anterior commissure remains comparable to controls at the midline. (F) *ntn1b* knock down embryo at 48 hpf. The ectopic axons are still visible ventral to the AC (thin arrow) and can be seen to clearly detach from the lateral margins of the commissure (arrowheads). Scale bars=25 μm at 30 hpf, 30 μm at 48 hpf.

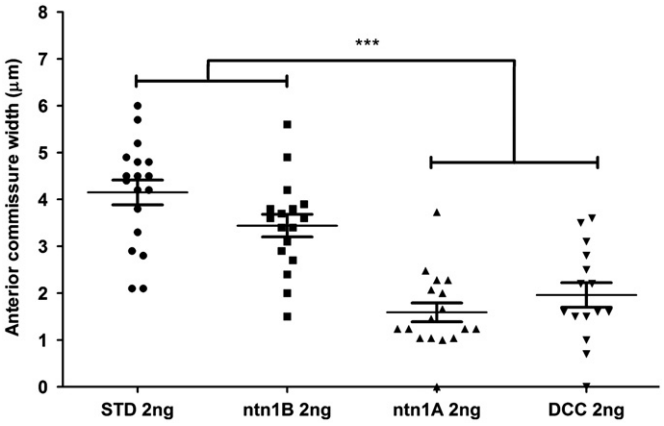

Fig. 9. *Knocking down either dcc or ntn1a, but not ntn1b, reduces the size of the anterior commissure at 30 hpf.* The bulk of the anterior commissure has been measured on maximum intensity projection confocal images at the midline on frontal views (as in Fig. 7). A one-way ANOVA analysis with a Tukey post-test test indicated that *dcc* and *ntn1a* MO knock downs exhibited a significant reduction of the anterior commissure compared to STD controls or *ntn1b* knock downs ($p < 0.001$).

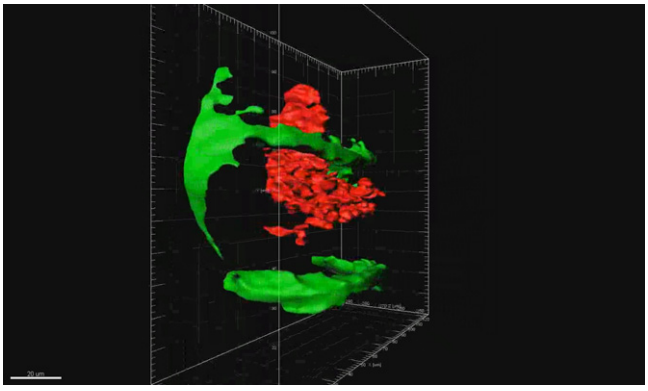

Movie S5. Supplementary movie 05. 3D reconstruction of the double labelling for *ntn1a* and acetylated tubulin shown in Fig. 10. http://dx.doi.org/10.1016/j.ydbio.2012.04.032.

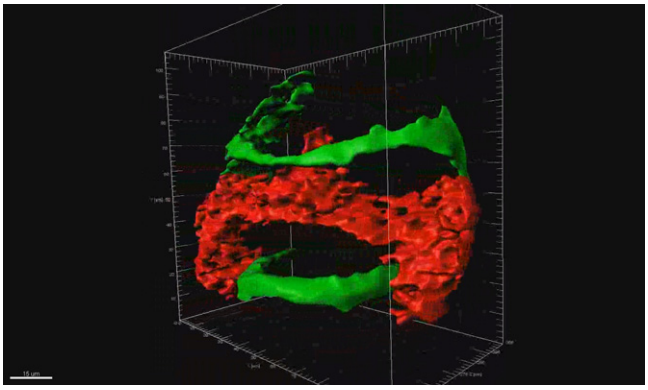

Movie S6. Supplementary movie 06. 3D reconstruction of the double labelling for *ntn1b* and acetylated tubulin shown in Fig. 10. http://dx.doi.org/10.1016/j.ydbio.2012.04.032.

commissure passes immediately rostral to the triangular wedge of *netrin1* expression (Fig. 9E and F). Interestingly, lateral views revealed that the anterior commissure appears to cross the midline in a shallow depression of the rostral surface of the *ntn1a* expression domain (dotted line, Fig. 9G). In contrast, the anterior commissure sits slightly above the dorsal surface of the *ntn1b* domain (arrowheads, Fig. 9H).

Taken together, these results indicate that *ntn1a* constitutes a good candidate for a long range signal for attracting remotely localised neurons expressing *dcc* in the dorsorostral cluster of neurons. This is in agreement with our results showing that synergistic interactions of *dcc* and *ntn1a* inhibit both the emergence of the EDAB and the reduced anterior commissure phenotype before 30 hpf. On the other hand, *ntn1b* appears to be more consistent with a role as chemorepellant since the ectopic axons observed in all *ntn1b* knock downs invade the neuroepithelium ventral to the anterior commissure, particularly from the lateral edge of the tract in the region where *ntn1b* is normally expressed.

Discussion

We show here that it is possible to induce growing axons to pioneer and establish a novel axon trajectory in the embryonic vertebrate forebrain by modulating the function of pre-existing guidance cues. Genetic manipulation of axon guidance cues typically either perturbs axon tract and commissure formation or causes abnormal axon fasciculation and mistargeting during development (Chédotal and Richards, 2010). However, we have demonstrated a highly selective gain-of-function phenotype with loss of either the chemoattractive receptor *dcc* and/or its ligand, *ntn1a*. By knocking down either *dcc* or *ntn1a* we are able to generate a novel bundle of axons which we refer to as the ectopic diencephalic axon bundle (EDAB). The axons in this bundle pioneer a pathway arising from the caudal region of the dorsocaudal cluster of neurons which form the presumptive telencephalon (Fig. 10) and strongly express *dcc*. These axons typically follow a stereotypical route through the ipsilateral diencephalon to the ventral rostral cluster (VRC, Fig. 10) of neurons. None of these features were observed when we knocked down *ntn1b*, the paralogue of *ntn1a*, indicating that the creation of this new axon bundle was very specific to interactions associated with only *ntn1a* and *dcc* Fig. 11.

The reduction in the size as well as aberrant midline crossing of the anterior commissure that we observed with knock down of either netrin1 paralogues or *dcc* in zebrafish is consistent with previous observations in mutant mice. Mice null mutant for either *Netrin1* (Serafini et al., 1996) or *Dcc* (Fazeli et al., 1997) exhibited serious commissural defects in the corpus callosum and the hippocampal and anterior commissures, while leaving the posterior and habenular commissures largely unaffected. Interestingly, loss of *Dcc* or *Netrin1* in mice caused a loss of the anterior limb of the anterior commissure and only a partially penetrant reduction in size of the posterior limb of the anterior commissure. We are the first to analyse the early development of the *dcc* and *netrin1* phenotypes and we confirmed the reduction of the early forming anterior commissure, which is equivalent to the posterior limb of the mature anterior commissure in mice (Jouandet and Hartenstein, 1983). The anterior limb of the anterior commissure, which interconnects the olfactory bulbs, develops later in zebrafish and was not analysed here. As in mice, we did not observe defects in the posterior and habenular commissures in zebrafish. The similarities of these phenotypes in two species separated by at least 400 million years (Nobrega and Pennacchio, 2004) highlights the fundamental importance of these guidance cues in the development of the vertebrate forebrain. Moreover, these results strongly support the specificity of the morpholino-based approach used here to manipulate gene expression.

The potential off-target effects of morpholinos are well documented today and several studies and reports warn against

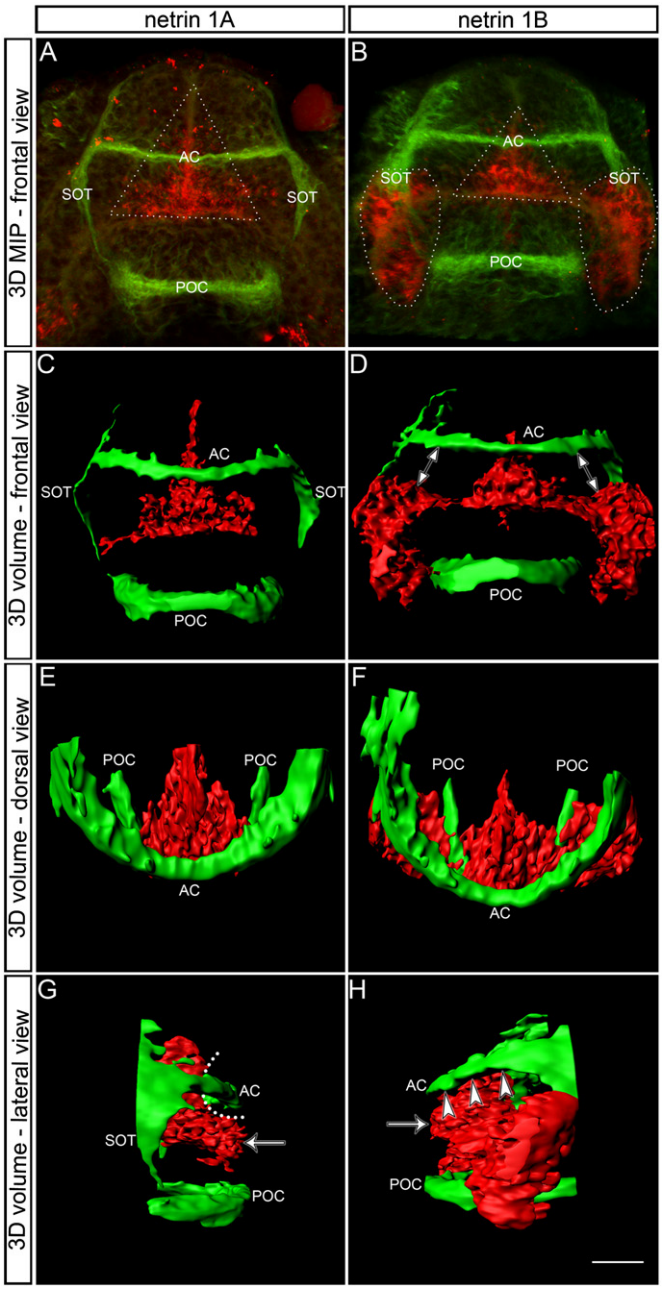

Fig. 10. *Expression patterns of ntn1a and ntn1b at the commissural plate. In situ* hydridization staining for expression of *netrin1a* (*ntn1a*) and *netrin1b* (*ntn1b*) is represented in red while immunostaining for axons is represented in green (various tracts are labelled according to Fig. 1). (A) and (B) are orthogonal maximum intensity projection of the native confocal stacks. (C)–(H) are 3-dimensional volume representations obtained using Imaris software. (A)–(D) Frontal views of rostral surface of the brain (commissural plate) (dorsal is up). (E)–(F) Dorsal views (anterior is down). (G) Lateral view (anterior is right). (H) Anterior view (anterior is left). Arrow in (G) and (H) represents anterior midline border between telencephalon and diencephalon. Scale bar=15 μm.

misinterpretation of experimental data collected while using morpholino knock down (for review see Eisen and Smith, 2008). The efficacy of all morpholinos used here had been demonstrated in previous studies (Suli et al., 2006; Kastenhuber et al., 2009; Lim et al., 2011; Nasevicius and Ekker, 2000). One of the main aspects of off-target effects with morpholinos is the triggering of unspecific cell-death via activation of the p53 pathway. High doses of morpholino generally cause such activation and results in gross defects that can considerably bias the interpretation of the data

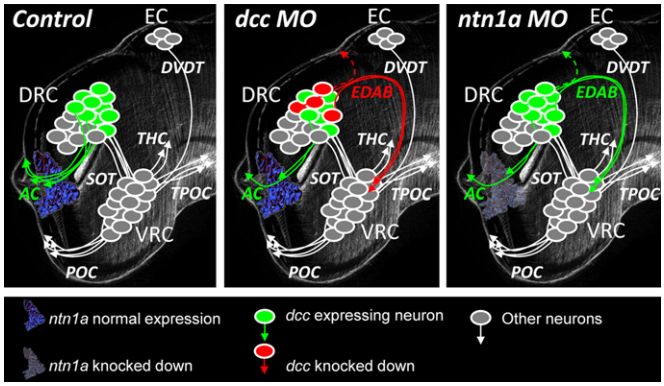

Fig. 11. *Overview of the emergence of the EDAB.* Control. Control embryos express *netrin1a* at the rostral midline (in blue). Axon tracts appear as in Fig. 1. A subpopulation of neurons located in the caudal part of the DRC and expressing *dcc* (green) project their axons into the anterior commissure. *dcc* MO. In a *dcc* knock down embryo, loss of *dcc* in DRC neurons causes a subpopulation of neurons (in red) that normal project rostrally to inappropriately project caudally and form the EDAB. These axons can cross the midline in 8% of the cases or project ventrally to the VRC in 92% of the cases. *ntn1a* MO. The loss of function of *netrin1a* (in grey) phenocopies the *dcc* knock down. The *dcc* expressing neurons of the caudal portion of the DRC (in green) project aberrantly to the diencephalon and form the EDAB.

(Robu et al., 2007). In the present study we made sure that the amount of morpholinos used was kept under the level of activation of unspecific cell death as revealed by an acridine orange staining protocol (Tucker and Lardelli, 2007). The specificity of the phenotype linked to the loss of function was also assessed by the use of 2 different morpholinos for *dcc* and the observation of similar phenotypes in only one paralogue of netrin 1 loss-of-function with a very similar dose–reponse curve. The synergisitc effect of both *dcc* and *ntn1a* morpholino at subthreshold further emphasised the specificity of the phenotype. A mosaic gain-of-*ntn1a*-function approach would provide further insight into the behaviour of *dcc* expressing neurons in this region of the brain.

Competing cues during axon guidance in the presumptive telencephalon

The expression pattern of *ntn1a* in the rostral midline of the commissural plate (this study) and *dcc* in the caudal portion of the dorsorostral cluster of neurons in the telencephalon (Supplementary Fig. 1; Hjorth et al., 2001) is consistent with *ntn1a* acting as a long-range chemoattractive ligand that guides these axons to the rostral midline during the establishment of the anterior commissure. Since the anterior commissure is not lost completely following loss-of-function of *dcc* or *netrin1* in either mice or zebrafish, it seems that the formation of this pathway is dependent on multiple guidance cues. This is understandable considering that this commissure is formed by a heterogenous population of neurons that terminate in multiple sites within the brain. When we suppressed the attraction of the caudally located (and *dcc* expressing) neurons to the rostral midline, it not only significantly reduced axons entering the anterior commissure, but it caused these telencephalic axons to ectopically extend caudally into the diencephalon, forming the EDAB. This shows that these *dcc*-expressing axons, once released from *ntn1a* attraction towards the rostral midline, are capable of responding to other cues; either repulsive cues located rostrally and/or attractive cues located caudally.

During normal development, *dcc* expressing axons do not terminate at the midline despite the presence of strong midline chemoattractive cues (Evans and Bashaw, 2010). The ability of axons to grow through the midline and enter the contralateral side of the brain has been partly attributed to their increased responsiveness to midline chemorepulsive cues. In the mouse

spinal cord, many commissural axons stall in their ventral trajectory and fail to reach the midline following loss of either *Dcc* or *Netrin1* (Serafini et al., 1996; Fazeli et al., 1997). These axons appear to be inhibited by their increased responsiveness to midline chemorepulsive slits (Evans and Bashaw, 2010). Interestingly, we did not observe this behaviour in the developing telencephalon in our *dcc* or *ntn1a* knock down zebrafish embryos. We cannot rule out the possibility that some axons originating from the caudal telencephalon wander within the telencephalic cluster without exiting either through the anterior commissure or the EDAB. However, our back tracing experiments showed that the EDAB axons did not initially grow towards the rostral midline and then stall or turnabout as if they responded to chemorepulsive ligands secreted from the midline. Instead, these axons initially grew caudally as if they were responding to local cues either in the dorsorostral cluster or more caudally in the dorsal diencephalon.

Due to the large number of potential candidate guidance cues, we only just started exploring the possibilities in the present study with *shh*. Hedgehog is expressed at the *zona limitans intrathalamica* (Scholpp et al., 2006). Knocking down *shh* did not rescue the EDAB phenotype in *dcc* morphants. But one should keep in mind that a hedgehog paralogue, *tiggy-winkle hedgehog* (*twhh*), is also expressed in this region and may as well play an attractive role for EDAB axons. Knocking down both hedgehog paralogues or using the smo mutant line would help to decipher the potential role of the hedgehog family in the EDAB guidance.

It should be noted that studies in *C. elegans* have shown a neuronal asymmetry inducing mechanism for *unc-6* (orthologue of vertebrate netrins) and *unc-40* (orthologue of the vertebrate dcc family) (Adler et al., 2006). The loss of function of either of these components delays the emergence of the axon, and eventually leads to misoriented and mistargeted axons. Both extension and polarity of protrusion can be mediated by *unc-6*/*unc-40* system via partially distinct mechanisms (Norris and Lundquist, 2011). We cannot rule out the possibility that *dcc*–*ntn1a* interactions may be acting both to polarise the initial rostral emergence of the axon as well as to subsequently steer the growth cone. However, one should keep in mind that the polarity inducing function described in the nematode has not yet been reported in vertebrates. The duplication of the ancestral genes into several copies found in vertebrates is very likely associated with a subfunctionalization of these different orthologues. It is more likely possible that while *unc-40* is mediating several functions in the nematode worms, *dcc* has a narrowed functional range in vertebrates due to the presence of other homologues in the DEAL family (Salbaum and Kappen, 2000; Takahashi et al., 2010).

Subfunctionalization of netrin1 paralogues

While our results support *ntn1a* acting as a chemoattractive cue for early growing *dcc*-expressing anterior commissural axons, *ntn1b* seems to instead exhibit a chemorepulsive role in the commissural plate. Loss of *ntn1b* caused a subpopulation of anterior commissural axons to divert from the tract as it approached the commissural plate. These axons dispersed aberrantly within the neuroepithelium lying ventral to the anterior commissure and dorsal to the telencephalic–diencephalic border. Since these misguided axons exited the tract of the anterior commissure as they reached the region where the lateral domain of *ntn1b* is normally expressed we have postulated that this netrin-1 paralogue is acting as a chemorepulsive cue to channel axons into the anterior commissure.

In vertebrates, netrin1 dependent chemorepulsion is mediated by a complex of Unc5 and Dcc (Hong et al., 1999). Since we did not observe the *ntn1b* phenotype in *dcc* knock downs it would appear that *unc5* may not play a role in this aberrant axon growth within the commissural plate. However, this conclusion may be too simplistic since the Dcc-expressing axons that form the EDAB may be the same subpopulation of axons that normally respond to Ntn1b in the rostral brain and grow aberrantly out of the tract of the anterior commissure. These axons never enter the anterior commissure in *dcc* knock downs because they form the EDAB. For this reason we cannot rule out the role of Unc5–Dcc interactions in the *ntn1b* phenotype. Understanding the receptors mediating Ntn1b signalling will be challenging considering that there are four subtypes of Unc5 receptors (A–D) as well as possible gene duplications within this family (Moore et al., 2007).

Conclusion

Using laser confocal microscopy and the power of 3-dimensional analyses afforded by the small size of the zebrafish embryonic brain we were able to visualise the cellular basis of loss-of-function axon guidance phenotypes at a resolution rarely achievable in higher vertebrates. We have shown that the neurons located in the dorsocaudal part of the telencephalic cluster of neurons normally project to the contralateral telencephalon via the anterior commissure (Fig. 10). These *dcc*-expressing neurons fail to project into the anterior commissure following loss of *dcc* or *ntn1a* and instead these axons follow a new caudoventral trajectory that projects to the ventrorostral cluster of neurons in the ventral diencephalon. Thus, we have established the principle that novel axon trajectories can be induced *de novo* in the early embryonic brain by manipulating the expression of endogenous axon guidance receptors and their ligands.

Role of the funding source

This work was supported by a project grant from the Australian Research Council awarded to B.K.

Appendix A. Supplementary material

Supplementary data associated with this article can be found in the online version at http://dx.doi.org/10.1016/j.ydbio.2012.04.032.

References

Adler, C.E., Fetter, R.D., Bargmann, C.I., 2006. UNC-6/Netrin induces neuronal asymmetry and defines the site of axon formation. Nat. Neurosci. 9, 511–518.
Anderson, R.B., Key, B., 1999. Novel guidance cues during neuronal pathfinding in the early scaffold of axon tracts in the rostral brain. Development 126, 1859–1868.
Charron, F., Stein, E., Jeong, J., McMahon, A.P., Tessier-Lavigne, M., 2003. The morphogen sonic hedgehog is an axonal chemoattractant that collaborates with netrin-1 in midline axon guidance. Cell 113, 11–23.
Chedotal, A., Richards, L.J., 2010. Wiring the brain: the biology of neuronal guidance. Cold Spring Harb. Perspect. Biol. 2, a001917.
Chitnis, A.B., Kuwada, J.Y., 1990. Axonogenesis in the brain of zebrafish embryos. J. Neurosci. 10, 1892–1905.
Cordell, H.J., 2002. Epistasis: what it means, what it doesn't mean, and statistical methods to detect it in humans. Hum. Mol. Genet. 11, 2463–2468.
Easter Jr., S.S., Ross, L.S., Frankfurter, A., 1993. Initial tract formation in the mouse brain. J. Neurosci. 13, 285–299.
Eisen, J.S., Smith, J.C., 2008. Controlling morpholino experiments: don't stop making antisense. Development 135, 1735–1743.
Evans, TA, Bashaw, GJ, 2010. Axon guidance at the midline: of mice and flies. Curr Opin Neurobiol 20, 79–85.
Fazeli, A., Dickinson, S.L., Hermiston, M.L., Tighe, R.V., Steen, R.G., Small, C.G., Stoeckli, E.T., Keino-Masu, K., Masu, M., Rayburn, H., Simons, J., Bronson, R.T., Gordon, J.I., Tessier-Lavigne, M., Weinberg, R.A., 1997. Phenotype of mice

lacking functional Deleted in colorectal cancer (Dcc) gene. Nature 386, 796–804.
Fearon, E.R., Cho, K.R., Nigro, J.M., Kern, S.E., Simons, J.W., Ruppert, J.M., Hamilton, S.R., Preisinger, A.C., Thomas, G., Kinzler, K.W., et al., 1990. Identification of a chromosome 18q gene that is altered in colorectal cancers. Science 247, 49–56.
Fricke, C., Chien, C.B., 2005. Cloning of full-length zebrafish dcc and expression analysis during embryonic and early larval development. Dev. Dyn 234, 732–739.
Gates, M.A., Kim, L., Egan, E.S., Cardozo, T., Sirotkin, H.I., Dougan, S.T., Lashkari, D., Abagyan, R., Schier, A.F., Talbot, W.S., 1999. A genetic linkage map for zebrafish: comparative analysis and localization of genes and expressed sequences. Genome Res. 9, 334–347.
Gilmour, D.T., Maischein, H.M., Nusslein-Volhard, C., 2002. Migration and function of a glial subtype in the vertebrate peripheral nervous system. Neuron 34, 577–588.
Guarente, L., 1993. Synthetic enhancement in gene interaction: a genetic tool come of age. Trends Genet 9, 362–366.
Hendricks, M., Jesuthasan, S., 2007. Asymmetric innervation of the habenula in zebrafish. J. Comp. Neurol. 502, 611–619.
Hjorth, J.T., Gad, J., Cooper, H., Key, B., 2001. A zebrafish homologue of deleted in colorectal cancer (zdcc) is expressed in the first neuronal clusters of the developing brain. Mech. Dev 109, 105–109.
Hjorth, J.T., Key, B., 2001. Are pioneer axons guided by regulatory gene expression domains in the zebrafish forebrain? High-resolution analysis of the patterning of the zebrafish brain during axon tract formation. Dev. Biol 229, 271–286.
Hong, K., Hinck, L., Nishiyama, M., Poo, M.M., Tessier-Lavigne, M., Stein, E., 1999. A ligand-gated association between cytoplasmic domains of UNC5 and DCC family receptors converts netrin-induced growth cone attraction to repulsion. Cell 97, 927–941.
Jouandet, M.L., Hartenstein, V., 1983. Basal telencephalic origins of the anterior commissure of the rat. Exp. Brain. Res. 50, 183–192.
Kassahn, K.S., Dang, V.T., Wilkins, S.J., Perkins, A.C., Ragan, M.A., 2009. Evolution of gene function and regulatory control after whole-genome duplication: comparative analyses in vertebrates. Genome Res. 19, 1404–1418.
Kastenhuber, E., Kern, U., Bonkowsky, J.L., Chien, C.B., Driever, W., Schweitzer, J., 2009. Netrin-*DCC*, Robo-Slit, and heparan sulfate proteoglycans coordinate lateral positioning of longitudinal dopaminergic diencephalospinal axons. J. Neurosci. 29, 8914–8926.
Keino-Masu, K., Masu, M., Hinck, L., Leonardo, E.D., Chan, S.S., Culotti, J.G., Tessier-Lavigne, M., 1996. Deleted in Colorectal Cancer (*DCC*) encodes a netrin receptor. Cell 87, 175–185.
Kemp, H.A., Carmany-Rampey, A., Moens, C., 2009. Generating chimeric zebrafish embryos by transplantation. J.Vis. Exp.
Kimmel, C.B., Ballard, W.W., Kimmel, S.R., Ullmann, B., Schilling, T.F., 1995. Stages of embryonic development of the zebrafish. Dev. Dyn. 203, 253–310.
Lauderdale, J.D., Davis, N.M., Kuwada, J.Y., 1997. Axon tracts correlate with netrin-1a expression in the zebrafish embryo. Mol. Cell. Neurosci. 9, 293–313.
Lawlor, K.G., Narayanan, R., 1992. Persistent expression of the tumor suppressor gene *DCC* is essential for neuronal differentiation. Cell. Growth. Differ. 3, 609–616.
Lim, A.H., Suli, A., Yaniv, K., Weinstein, B., Li, D.Y., Chien, C.B., 2011. Motoneurons are essential for vascular pathfinding. Development 138, 3847–3857.
Macdonald, R., Scholes, J., Strähle, U., Brennan, C., Holder, N., Brand, M., Wilson, S.W., 1997. The Pax protein Noi is required for commissural axon pathway formation in the rostral forebrain. Development 124, 2397–2408.
Meyer, A., Malaga-Trillo, E., 1999. Vertebrate genomics: More fishy tales about Hox genes. Current biology 9, R210–213.
Moore, S., Tessier-Lavigne, M., Kennedy, T., 2007. Netrins and their receptors. In: Axon Growth and Guidance Advances in Experimental Medicine and Biology, 2007, vol. 621, pp. 17–31.
Moulton, J.D., Yan, Y.L., 2008. Using Morpholinos to control gene expression. Curr. Protoc. Mol. Biol. Chapter 26, Unit 26, 8.
Nasevicius, A., Ekker, S.C., 2000. Effective targeted gene 'knockdown' in zebrafish. Nat. Genet. 26, 216–220.
Nobrega, M.A., Pennacchio, L.A., 2004. Comparative genomic analysis as a tool for biological discovery. J. Physiol. 554, 31–39.
Norris, A.D., Lundquist, E.A., 2011. UNC-6/netrin and its receptors UNC-5 and UNC-40/*DCC* modulate growth cone protrusion *in vivo* in C. elegans. Development 138, 4433–4442.
Park, K.W., Urness, L.D., Senchuk, M.M., Colvin, C.J., Wythe, J.D., Chien, C.B., Li, D.Y., 2005. Identification of new netrin family members in zebrafish: developmental expression of netrin 2 and netrin 4. Dev. Dyn. 234, 726–731.
Postlethwait, J.H., 2007. The zebrafish genome in context: ohnologs gone missing. J. Exp. Zool. B. Mol. Dev. Evol 308, 563–577.
Prykhozhij, S.V., 2010. In the absence of Sonic hedgehog, p53 induces apoptosis and inhibits retinal cell proliferation, cell-cycle exit and differentiation in zebrafish. PLoS One 5, e13549.
Robu, M.E., Larson, J.D., Nasevicius, A., Beiraghi, S., Brenner, C., Farber, S.A., Ekker, S.C., 2007. p53 activation by knockdown technologies. PLoS Genet 3, e78.
Ross, L.S., Parrett, T., Easter Jr., S.S., 1992. Axonogenesis and morphogenesis in the embryonic zebrafish brain. J. Neurosci. 12, 467–482.
Salbaum, J.M., Kappen, C., 2000. Cloning and expression of nope, a new mouse gene of the immunoglobulin superfamily related to guidance receptors. Genomics 64, 15–23.
Sato, T., Takahoko, M., Okamoto, H., 2006. HuC:Kaede, a useful tool to label neural morphologies in networks *in vivo*. Genesis 44, 136–142.
Scholpp, S., Wolf, O., Brand, M., Lumsden, A., 2006. Hedgehog signalling from the zona limitans intrathalamica orchestrates patterning of the zebrafish diencephalon. Development 133, 855–864.
Serafini, T., Colamarino, S.A., Leonardo, E.D., Wang, H., Beddington, R., Skarnes, W.C., Tessier-Lavigne, M., 1996. Netrin-1 is required for commissural axon guidance in the developing vertebrate nervous system. Cell 87, 1001–1014.
Sperry, R.W., 1963. Chemoaffinity in the Orderly Growth of Nerve Fiber Patterns and Connections. Proc. Natl. Acad. Sci. USA 50, 703–710.
Strähle, U., Fischer, N., Blader, P., 1997. Expression and regulation of a netrin homologue in the zebrafish embryo. Mech. Dev. 62, 147–160.
Suli, A., Mortimer, N., Shepherd, I., Chien, C.B., 2006. Netrin/*DCC* signaling controls contralateral dendrites of octavolateralis efferent neurons. J. Neurosci. 26, 13328–13337.
Takahashi, K.F., Kiyoshima, T., Kobayashi, I., Xie, M., Yamaza, H., Fujiwara, H., Ookuma, Y., Nagata, K., Wada, H., Sakai, T., Terada, Y., Sakai, H., 2010. Protogenin, a new member of the immunoglobulin superfamily, is implicated in the development of the mouse lower first molar. BMC. Dev. Biol. 10, 115.
Tessier-Lavigne, M., Goodman, C.S., 1996. The molecular biology of axon guidance. Science 274, 1123–1133.
Tucker, B., Lardelli, M., 2007. A rapid apoptosis assay measuring relative acridine orange fluorescence in zebrafish embryos. Zebrafish 4, 113–116.
Valnes, K., Brandtzaeg, P., 1985. Retardation of immunofluorescence fading during microscopy. J. Histochem. Cytochem. 33, 755–761.
Ware, M., Schubert, F.R., 2011. Development of the early axon scaffold in the rostral brain of the chick embryo. J. Anat 219, 203–216.
Wilson, S.W., Ross, L.S., Parrett, T., Easter Jr., S.S., 1990. The development of a simple scaffold of axon tracts in the brain of the embryonic zebrafish, Brachydanio rerio. Development 108, 121–145.